

Influence of annealing on the bias voltage dependence of tunneling magnetoresistance in MgO double-barrier magnetic tunnel junctions with CoFeB electrodes

Gen Feng, Sebastiaan van Dijken,^{a)} and J. M. D. Coey
CRANN and School of Physics, Trinity College, Dublin 2, Ireland

(Received 22 June 2006; accepted 30 August 2006; published online 16 October 2006)

Double-barrier magnetic tunnel junctions with two MgO barriers and three CoFeB layers exhibiting tunneling magnetoresistance (TMR) values of more than 100% were fabricated. The bias voltage dependence of the TMR ratio is highly asymmetric after annealing at low temperatures, indicating dissimilar CoFeB/MgO interfaces. The TMR effect decays very slowly for positive bias and is only reduced to half of its maximum value at $V_{1/2}=1.88$ V when the junctions are processed at 200 °C. The largest output voltage, 0.62 V, is obtained after annealing at 300 °C, a temperature that combines high TMR ratios with a considerable asymmetric bias dependence. © 2006 American Institute of Physics. [DOI: 10.1063/1.2362977]

Following the demonstration of large tunneling magnetoresistance (TMR) ratios and low resistance-area products in magnetic tunnel junctions with a crystalline MgO(001) barrier, MgO is now considered as the key barrier material for next-generation device applications. Giant TMR ratios well above 100% at room temperature have been obtained with epitaxial Fe/MgO/Fe junctions,¹⁻⁵ textured magnetic tunnel junctions (MTJs),⁶ and CoFeB/MgO/CoFeB structures.⁷⁻¹¹ In the latter case, the MgO barrier grows with a highly oriented (001) texture on top of an amorphous CoFeB layer. A postdeposition annealing process then crystallizes the CoFeB electrodes, thereby creating the different Bloch state symmetries with dissimilar decay rates in the MgO barrier that are necessary for giant TMR values.^{12,13} In practical applications, MTJ structures are biased to increase the output voltage and decrease its signal-to-noise ratio. Electronic structure effects, magnon excitations, and spin-flip scattering on interface defects, however, reduce the TMR effect at elevated bias voltage and this limits the output signal of MTJ sensors and memory elements. A possible solution is to use double-barrier magnetic tunnel junctions (DMTJs) where the applied voltage is divided over two single junctions. Experimental studies on DMTJs with amorphous Al₂O₃ barriers¹⁴⁻¹⁶ and fully epitaxial Fe/MgO double-barrier structures¹⁷ have indeed confirmed a slower decay of the TMR ratio with bias voltage. In this letter, we demonstrate that high quality double-barrier junctions with crystalline MgO barriers and CoFeB electrodes can be fabricated by magnetron sputtering and postdeposition annealing. The bias voltage dependence of the TMR is asymmetric and depends strongly on the annealing temperature. These results can be used to engineer MTJs with high output signals.

The DMTJs consisting of a 5 Ta/50 Ru/5 Ta/5 NiFe/10 IrMn/2 CoFe/0.7 Ru/4 CoFeB/2.5 MgO/3 CoFeB/2.5 MgO/4 CoFeB/0.7 Ru/2 CoFe/10 IrMn/5 NiFe/5 Ta (thickness in nanometers) multilayer stack were grown by magnetron sputtering on thermally oxidized Si substrates in our Shamrock deposition tool. All metallic layers were deposited by dc sputtering and a Co₄₀Fe₄₀B₂₀ (at. %) alloy target was used

for the ferromagnetic electrodes. The MgO barriers were fabricated by rf sputtering from two MgO targets in a target-facing-target gun. After deposition, the multilayer stacks were patterned into 20×20 to 100×100 μm² junctions by UV lithography and subsequently annealed for 90 min in vacuum at temperatures ranging from 200 to 375 °C. During annealing a magnetic field of 0.8 T was applied to establish uniform exchange bias in the electrodes.¹⁸ The structure of the layers in the DMTJ stack was characterized by x-ray diffraction. Whereas the MgO barriers already exhibit a clear (001) texture after deposition, the CoFeB electrodes were found to crystallize into a bcc(001) structure upon annealing. The magnetic and magnetotransport properties of the DMTJs were measured using an alternating gradient force magnetometer (AGM) and a four-probe method where the polarity of the bias voltage is defined with respect to the top electrode. For comparison, single-barrier magnetic tunnel junctions (SMTJs) with a 5 Ta/50 Ru/5 Ta/5 NiFe/10 IrMn/2 CoFe/0.7 Ru/3 CoFeB/2.5 MgO/5 CoFeB/5 NiFe/5 Ta structure were also fabricated.

As-deposited DMTJs only exhibit a TMR of about 20%, which is due to a lack of bias in the bottom reference layer and the amorphous structure of the CoFeB electrodes in which the Δ₁ bands responsible for high TMR ratios are absent. After vacuum annealing at 325 °C, the moments of the ferromagnetic layers reverse at distinctive applied magnetic fields. The AGM measurement of the continuous multilayer stack [Fig. 1(a)] indicates that the free CoFeB layer between the two MgO barriers switches in small applied fields and that the bottom and top CoFeB reference layers exhibit biases of 40 and 16 mT, respectively. The inactive layers in terms of magnetotransport reverse at positive applied magnetic fields. This, together with a crystallization of the CoFeB electrodes, results in a TMR effect of 105% at room temperature [Fig. 1(b)]. The RA product of the DMTJ junctions is 5×10⁶ Ω μm², which is about twice the RA product of the SMTJ, indicating that electron transport in the DMTJ is characterized by sequential tunneling events and that the DMTJ structure can be regarded as a serial connection of two single tunnel junctions. In this tunneling regime, the TMR ratio of the DMTJ cannot exceed the largest TMR value of the two single barriers.¹⁹ Sequential tunneling in our

^{a)}Electronic mail: bas_vandijken@yahoo.com

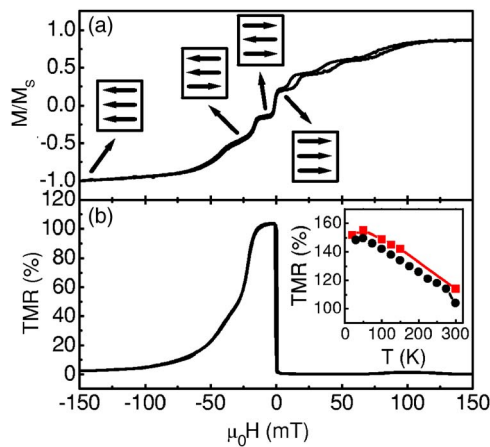


FIG. 1. (Color online) (a) Magnetization and (b) TMR vs field curves for the DMTJ stack after annealing at 325 °C. The arrows in (a) indicate the orientation of the CoFeB magnetic moments. The inset in (b) depicts the temperature dependence of the TMR effect in single-barrier (red squares) and double-barrier (black circles) junctions.

DMTJs is also confirmed by the temperature dependence of the TMR effect [see inset of Fig. 1(b)]. For the DMTJ, the TMR ratio increases from 105% at 300 K to 149% at 50 K. This behavior is qualitatively similar to that of the SMTJ exhibiting a TMR increase from 114% to 155%. A stronger TMR temperature dependence is only expected when electron transport in the middle ferromagnetic layer is phase coherent, something that is obviously not the case for the 3 nm thick CoFeB middle electrode in our stack.

Figure 2 shows DMTJ TMR curves after annealing for 90 min at different temperatures (T_A). Well-separated switching of the magnetic moments is obtained for an annealing temperature of up to 350 °C. In this range, the TMR ratio increases with annealing temperature due to a crystallization of the CoFeB electrodes into a bcc structure with a preferred (001) orientation. Annealing at 375 °C leads to a breakdown of exchange bias and consequently to a drastic decrease of the TMR effect. As indicated by the minor TMR curves in

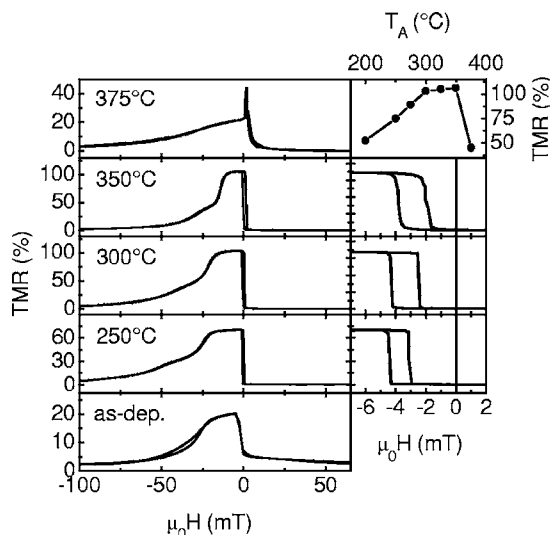


FIG. 2. DMTJ TMR curves for the as-deposited stack and after annealing at different temperatures. The upper right panel depicts the annealing temperature dependence of the TMR ratio. The other right panels show minor TMR vs field curves indicating a small negative bias in the reversal fields of the free CoFeB electrode.

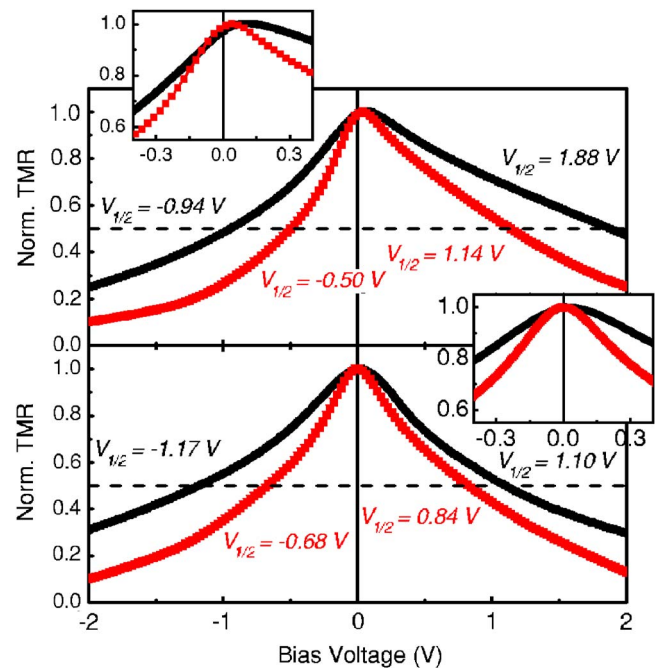


FIG. 3. (Color online) Normalized TMR vs bias voltage curves for DMTJ (black circles) and SMTJ (red squares) structures. The data in the upper and lower panels were obtained after annealing at 200 and 350 °C, respectively. The insets show detailed measurements on the same junctions at small bias.

the right panels of Fig. 2, magnetization reversal in the free CoFeB layer is slightly shifted to negative applied fields and the magnitude of this offset depends on the annealing temperature. At $T_A=200$ °C the offset amounts to -4.2 mT and it decreases to -2.8 mT after annealing at 350 °C. The hysteresis loop shift, which is detrimental to practical applications, is predominantly due to Néel orange peel coupling between the CoFeB electrodes.^{20,21} This magnetostatic effect is associated with conformal roughness in the ferromagnetic electrodes and is generally found to be strongest for rough magnetic tunnel barrier interfaces.²² The decrease of the coupling field in our DMTJ structures with increasing annealing temperature therefore suggests that annealing at elevated temperatures not only crystallizes the CoFeB electrodes but also smoothens the CoFeB/MgO interfaces.

The bias voltage dependence of the TMR in the DMTJ and SMTJ structures after annealing at 200 and 350 °C is depicted in Fig. 3. Annealing at a moderate temperature of 200 °C results in an asymmetrical variation of the TMR ratio with applied bias. In addition, the bias voltages for which the TMR ratio is reduced to half of its maximum ($\pm V_{1/2}$) are considerably larger for DMTJs than for SMTJs, which is explained by a division of the applied voltage between two single barriers. The value of $+V_{1/2}=1.88$ V for the DMTJ structure is, to our knowledge, the largest value ever reported. The asymmetry in the TMR versus bias voltage reflects dissimilar CoFeB/MgO interfaces in the moderately annealed DMTJ stacks. For epitaxial Fe/MgO/Fe junctions an asymmetry in the bias voltage dependence of the TMR ratio has also been found and this was attributed to different dislocation densities at the top and bottom Fe/MgO interfaces and interfacial resonance states in the Fe minority spin band.^{1,3,5} The CoFeB electrodes, on the other hand, are amorphous in the as-deposited state and annealing at 200 °C only induces a partial crystallization. The asymmetry in our CoFeB/MgO/CoFeB single- and double-barrier junctions is

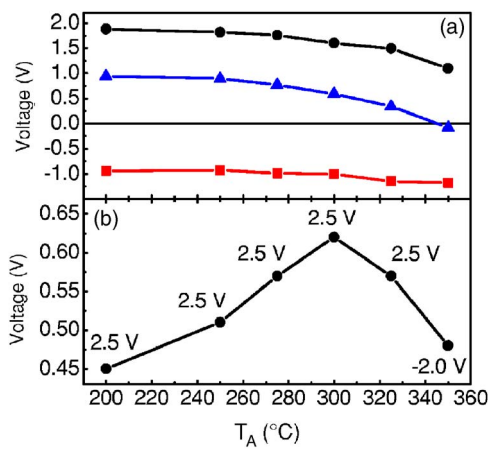


FIG. 4. (Color online) (a) $+V_{1/2}$ (black circles) and $-V_{1/2}$ (red squares) values for the DMTJ structures as a function of annealing temperature. The blue triangles indicate the asymmetry in the bias voltage dependence of the TMR [$(+V_{1/2}) - (-V_{1/2})$]. (b) Maximum output voltage of the DMTJs as a function of annealing temperature. The values in the plot indicate the bias voltage for which the output voltage is largest.

therefore most likely due to different structural defect densities at the CoFeB/MgO interfaces as a result of dissimilar crystallization rates in the CoFeB electrodes. This interpretation is supported by other experiments indicating a dependence of the crystallization process on CoFeB layer thickness and adjacent film structures.^{10,23} In addition to the asymmetry in the $+V_{1/2}$ and $-V_{1/2}$ values, the DMTJ and SMTJ also exhibit a shift of the TMR maximum to positive bias voltages of 10 and 4 mV, respectively. This offset reflects an initially larger increase of the tunneling conductance with positive applied bias for a parallel than for an antiparallel alignment of the magnetic moments.

The observed asymmetry and shift in the bias voltage dependence of the TMR gradually decrease with increasing annealing temperature [see Fig. 4(a)]. Annealing the DMTJ stack at 350 °C results in a nearly symmetrical TMR versus bias voltage curve with $-V_{1/2} = -1.17$ V and $+V_{1/2} = 1.10$ V. These values are much larger than those for the SMTJ, and the fact that the DMTJ exhibits a small but inversed asymmetry with respect to the SMTJ suggests that the two MgO tunnel barriers in the DMTJ have opposite TMR- V dependences. From this we conclude that although small dissimilarities between the CoFeB/MgO interfaces do still exist, the quality of the CoFeB/MgO interfaces in terms of roughness, structural defects, and the degree of CoFeB crystallization improves considerably upon annealing at elevated temperatures. A reduction of the CoFeB/MgO interface roughness qualitatively agrees with the observed decrease of the Néel orange peel coupling between the CoFeB electrodes with increasing annealing temperature (Fig. 2).

For sensor and memory applications, the variation of the MTJ output voltage, $V_{\text{out}} = V(R_{\text{AP}} - R_{\text{P}})/R_{\text{AP}}$, is an important parameter. Figure 4(b) summarizes the maximum output voltage as a function of annealing temperature. Unlike the TMR, the largest output voltage, $V_{\text{out,max}} = 0.62$ V, is obtained after annealing at 300 °C instead of 350 °C. This difference is due to a slow decay of the $(R_{\text{AP}} - R_{\text{P}})/R_{\text{AP}}$ ratio with positive bias voltage at low annealing temperatures. The magnitude of the maximum output voltage of the DMTJ is larger than those reported for fully epitaxial Fe/MgO/Fe

single-^{1,4} and double-barrier junctions¹⁷ as well as the $V_{\text{out,max}}$ obtained with CoFeB/MgO/CoFeB SMTJs.^{7,9-11} The data of Fig. 4 clearly show that a maximum output signal is obtained after annealing at a temperature for which the asymmetry in the bias voltage dependence of the TMR is still significant. This feature can be used to optimize the output voltage of MTJs in practical applications.

In summary, we have fabricated double-barrier MgO tunnel junctions with CoFeB electrodes. These structures are characterized by (1) large TMR ratios of more than 100% at room temperature, (2) a highly asymmetric bias voltage dependence of the TMR and a very large $+V_{1/2}$ value of 1.88 V after annealing at 200 °C, (3) a gradual decrease of this asymmetry and a reduction of the Néel coupling between the CoFeB electrodes with increasing annealing temperature, and (4) a maximum output voltage of 0.62 V after annealing at 300 °C, a temperature high enough for large TMR ratios but insufficient to remove the asymmetry from the bias dependence of the TMR effect.

This work was supported by Science Foundation Ireland.

- ¹S. Yuasa, T. Nagahama, A. Fukushima, Y. Suzuki, and K. Ando, *Nat. Mater.* **3**, 868 (2004).
- ²S. Yuasa, T. Katayama, T. Nagahama, A. Fukushima, H. Kubota, Y. Suzuki, and K. Ando, *Appl. Phys. Lett.* **87**, 222508 (2005).
- ³Y. Ando, T. Miyakoshi, M. Oogane, T. Miyazaki, H. Kubota, K. Ando, and S. Yuasa, *Appl. Phys. Lett.* **87**, 142502 (2005).
- ⁴C. Tiusan, F. Greullet, M. Sicot, M. Hehn, C. Bellouard, F. Montaigne, S. Andrieu, and A. Schuhl, *Appl. Phys. Lett.* **99**, 08A903 (2006).
- ⁵C. Tiusan, M. Sicot, J. Faure-Vincent, M. Hehn, C. Bellouard, F. Montaigne, S. Andrieu, and A. Schuhl, *J. Phys.: Condens. Matter* **18**, 941 (2006).
- ⁶S. S. P. Parkin, C. Kaiser, A. Panchula, P. M. Rice, B. Hughes, M. Samant, and S.-H. Yang, *Nat. Mater.* **3**, 862 (2004).
- ⁷D. D. Djayaprawira, K. Tsunekawa, M. Nagai, H. Maehara, S. Yuasa, Y. Suzuki, and K. Ando, *Appl. Phys. Lett.* **86**, 092502 (2005).
- ⁸K. Tsunekawa, D. D. Djayaprawira, M. Nagai, H. Maehara, S. Yamagata, S. Yuasa, Y. Suzuki, and K. Ando, *Appl. Phys. Lett.* **87**, 072503 (2005).
- ⁹G.-X. Miao, K. B. Chetry, A. Gupta, W. H. Butler, K. Tsunekawa, D. Djayaprawira, and G. Xiao, *J. Appl. Phys.* **99**, 08T305 (2006).
- ¹⁰C. Park, J.-G. Zhu, M. T. Moneck, Y. Peng, and D. E. Laughlin, *J. Appl. Phys.* **99**, 08A901 (2006).
- ¹¹S. Ikeda, J. Hayakawa, Y. M. Lee, T. Tanikawa, F. Matsukura, and H. Ohno, *J. Appl. Phys.* **99**, 08A907 (2006).
- ¹²W. H. Butler, X.-G. Zhang, T. C. Schulthess, and J. M. MacLaren, *Phys. Rev. B* **63**, 054416 (2001).
- ¹³X.-G. Zhang and W. H. Butler, *Phys. Rev. B* **70**, 172407 (2004).
- ¹⁴F. Montaigne, J. Nassar, A. Vaurès, F. Nguyen Van Dau, F. Petroff, A. Schuhl, and A. Fert, *Appl. Phys. Lett.* **73**, 2829 (1998).
- ¹⁵Y. Saito, M. Amano, K. Nakajima, S. Takahashi, M. Sagoi, and K. Inomata, *IEEE Trans. Magn.* **37**, 1979 (2001).
- ¹⁶S. Colis, G. Gieres, L. Bär, and J. Wecker, *Appl. Phys. Lett.* **83**, 948 (2003).
- ¹⁷T. Nozaki, A. Hirohata, N. Tezuka, S. Sugimoto, and K. Inomata, *Appl. Phys. Lett.* **86**, 082501 (2005).
- ¹⁸E. Kerr, S. van Dijken, and J. M. D. Coey, *J. Appl. Phys.* **97**, 093910 (2005).
- ¹⁹Z. P. Niu, Z. B. Feng, J. Yang, and D. Y. Xing, *Phys. Rev. B* **73**, 014432 (2006).
- ²⁰J. C. S. Kools, W. Kula, D. Mauri, and T. Lin, *J. Appl. Phys.* **85**, 4466 (1999).
- ²¹B. D. Schrag, A. Anguelouch, S. Ingvarsson, G. Xiao, Y. Lu, P. L. Trouiloud, A. Gupta, R. A. Wanner, W. J. Gallagher, P. M. Rice, and S. S. P. Parkin, *Appl. Phys. Lett.* **77**, 2373 (2000).
- ²²J. Kanak, T. Stobiecki, O. Schebaum, G. Reiss, and H. Brückl, *Phys. Status Solidi B* **243**, 197 (2006).
- ²³S. Yuasa, Y. Suzuki, T. Katayama, and K. Ando, *Appl. Phys. Lett.* **87**, 242403 (2005).